AMERICAN SOCIETY FOR MICROBIOLOGY | Journal of Bacteriology®

MEETING PRESENTATION

Role of *Caulobacter* Cell Surface Structures in Colonization of the Air-Liquid Interface

Aretha Fiebig[a]*

[a]Department of Biochemistry and Molecular Biology, The University of Chicago, Chicago, Illinois, USA

ABSTRACT In aquatic environments, *Caulobacter* spp. can be found at the boundary between liquid and air known as the neuston. I report an approach to study temporal features of *Caulobacter crescentus* colonization and pellicle biofilm development at the air-liquid interface and have defined the role of cell surface structures in this process. At this interface, *C. crescentus* initially forms a monolayer of cells bearing a surface adhesin known as the holdfast. When excised from the liquid surface, this monolayer strongly adheres to glass. The monolayer subsequently develops into a three-dimensional structure that is highly enriched in clusters of stalked cells known as rosettes. As this pellicle film matures, it becomes more cohesive and less adherent to a glass surface. A mutant strain lacking a flagellum does not efficiently reach the surface, and strains lacking type IV pili exhibit defects in organization of the three-dimensional pellicle. Strains unable to synthesize the holdfast fail to accumulate at the boundary between air and liquid and do not form a pellicle. Phase-contrast images support a model whereby the holdfast functions to trap *C. crescentus* cells at the air-liquid boundary. Unlike the holdfast, neither the flagellum nor type IV pili are required for *C. crescentus* to partition to the air-liquid interface. While it is well established that the holdfast enables adherence to solid surfaces, this study provides evidence that the holdfast has physicochemical properties that allow partitioning of nonmotile mother cells to the air-liquid interface and facilitate colonization of this microenvironment.

IMPORTANCE In aquatic environments, the boundary at the air interface is often highly enriched with nutrients and oxygen. Colonization of this niche likely confers a significant fitness advantage in many cases. This study provides evidence that the cell surface adhesin known as a holdfast enables *Caulobacter crescentus* to partition to and colonize the air-liquid interface. Additional surface structures, including the flagellum and type IV pili, are important determinants of colonization and biofilm formation at this boundary. Considering that holdfast-like adhesins are broadly conserved in *Caulobacter* spp. and other members of the diverse class *Alphaproteobacteria*, these surface structures may function broadly to facilitate colonization of air-liquid boundaries in a range of ecological contexts, including freshwater, marine, and soil ecosystems.

KEYWORDS *Alphaproteobacteria*, *Caulobacter*, biofilm, flagellum, holdfast, neuston, pellicle, type 4 pilus, unipolar polysaccharide

In aqueous systems, macronutrients partition to and accumulate at surfaces at both solid-liquid and air-liquid boundaries (1, 2), and dissolved oxygen levels are highest at air interfaces. An ability to take advantage of elevated concentrations of nutrients and/or oxygen at such surface boundaries likely confers a significant growth advantage in many cases (3). Certainly, bacteria have long been noted to partition to submerged solid surfaces (4, 5) and to air-liquid interfaces (6). Diverse morphological and metabolic characteristics of bacterial cells enable colonization of surface microenvironments.

Citation Fiebig A. 2019. Role of *Caulobacter* cell surface structures in colonization of the air-liquid interface. J Bacteriol 201:e00064-19. https://doi.org/10.1128/JB.00064-19.

Editor George O'Toole, Geisel School of Medicine, Dartmouth

Address correspondence to fiebigar@msu.edu.

* Present address: Department of Microbiology and Molecular Genetics, Michigan State University, East Lansing, Michigan, USA.

Received 17 January 2019
Accepted 15 April 2019
Accepted manuscript posted online 22 April 2019
Published 22 August 2019

As aquatic systems cover the majority of our planet, microbial activity in surface films has a significant impact on global biogeochemical cycles (7–10). Moreover, ecologically important aqueous interfaces are also found in terrestrial soils, where microbes occupy primarily the aqueous phase at solid- and air-liquid boundaries (10, 11). In porous soils and highly aerated bodies of water, bubbles provide mobile air-liquid surfaces upon which bacteria can be transported (10, 11). Though biofilms at air-liquid interfaces are not as well studied as solid surfaces, common themes in biofilm development in many species on varied surfaces have emerged over the past 2 decades. For example, flagellar motility and extracellular polysaccharides are important for colonization of both solid surfaces and air-liquid interfaces. In many cases, protein polymers, such as pili and curli, or extracellular DNA also plays a role in surface attachment and/or biofilm development (for reviews, see references 12 to 17).

Dimorphic bacterial model system to study colonization of the air-liquid interface. *Caulobacter* spp. are found in nearly any environment that experiences extended periods of moisture, including marine, freshwater, and soil ecosystems (18, 19). Poindexter previously reported an approach to enrich *Caulobacter* spp. by sampling from the air-liquid interface (20). Specifically, she noted that when natural water samples are left to stand, a pellicle enriched with prosthecate (i.e., stalked) bacteria will form at the surface, where liquid meets the air. *Caulobacter* has a dimorphic life cycle characteristic of many *Alphaproteobacteria* in which each cell division yields a motile newborn swarmer cell and a sessile mother cell (20–22). In the case of *Caulobacter*, the sessile mother cell has a polar prosthecum, or stalk, while the swarmer cell has a single flagellum and multiple type IV pili at one cell pole. The swarmer cell further has the capacity to secrete a polar adhesin, called a holdfast, at its flagellated/piliated pole (23–25). Cells are motile for only a fraction of the cell cycle; swarmers transition to sessile stalked cells upon initiation of DNA replication and thus undergo a transition from motile to sessile with every round of cell division.

As a swarmer cell transitions to a stalked cell, the flagellum is shed, and the pili are retracted, but the holdfast remains on the old pole from which the stalk emerges. In *Caulobacter crescentus*, the flagellum and pili are important for initial surface attachment, while the holdfast is required for permanent attachment to a range solid surfaces, including glass, mica, plastics, and decaying biotic material (23, 26). In fact, robust surface attachment via the holdfast adhesin is the characteristic that initially led to the isolation of *Caulobacter* species (27, 28). The holdfast also mediates polar cell-cell attachments resulting in the generation of multicellular structures, often called rosettes.

While the chemical composition of the holdfast material is not well understood, genetic and biochemical analyses indicate that it is a polysaccharide (29, 30) that contains four major sugars (31, 32). There is also evidence that protein and DNA are important components of this adhesin (33). The role of the *C. crescentus* holdfast and other surface structures, including the flagellum and type IV pili, in the colonization of the air-liquid interface has not been investigated.

In this study, I describe the process by which *C. crescentus* colonizes the air-liquid interface under static growth conditions and define molecular determinants of this colonization process. Initially, cells accumulate as individual cells evenly dispersed in a monolayer at the air-liquid interface. At sufficiently high density, the monolayer transitions to a dense multilayered pellicle structure composed primarily of large connected rosette aggregates. Polar cell surface appendages, including the flagellum, type IV pili, and the holdfast, all contribute to the development of this *C. crescentus* pellicle. As in biofilm formation on solid substrates, the flagellum and pili are important for efficient pellicle biofilm development, though neither is strictly required. Holdfast biosynthesis, on the other hand, is absolutely required for *C. crescentus* cells to accumulate at the air-liquid boundary and to form a pellicle. This work establishes a critical ecological role for the holdfast adhesin, namely, in partitioning of cells to the air-liquid interface. Moreover, this work establishes the pellicle as a system to study biofilm development in *C. crescentus* that is complementary to biofilm studies on solid surfaces.

RESULTS

***Caulobacter crescentus* forms a pellicle under static growth conditions.** To measure attachment to solid surfaces, bacteria are typically grown in polystyrene microtiter dishes or glass culture tubes, and surface-attached bacteria are detected by staining with crystal violet. When grown in static culture (i.e., without shaking), *C. crescentus* cells accumulate in high numbers on glass or polystyrene near the air-liquid interface (see Fig. 1B, bottom panel). This may reflect a bias in surface colonization at the boundary where the solid surface, culture medium, and air meet. Indeed, bacteria at this interface are reported to undergo rapid, irreversible attachment to solid surfaces at a level that is higher than that of cells in the bulk (10). However, it may also be the case that the enrichment of *C. crescentus* cells at the solid-liquid-air boundary simply reflects biased colonization of the entire air-liquid interface at the surface of the growth medium.

To visualize and monitor colonization of the air-liquid interface, I grew wild-type *C. crescentus* strain CB15 statically in large volumes of a peptone-yeast extract (PYE) broth. A recent genome-scale analysis of *C. crescentus* indicates that complex media, such as PYE, are a more ecologically relevant cultivation environment than a mineral defined medium, such as M2 (34). Under these conditions, as culture density increased, cells formed a surface film, or pellicle, that evenly covered the entire air-liquid interface (Fig. 1A). Growth was required for pellicle formation: cultures grown to stationary phase in a roller or shaker did not form pellicles when transferred to static conditions unless they were diluted with fresh growth medium (Fig. 1B). Static growth was accompanied by the establishment of a steep oxygen gradient in the culture flask. Dissolved oxygen levels were saturated in sterile growth medium across the measured depth of the culture flask. In contrast, oxygen was measurable in only the first 2 to 3 mm from the air-liquid interface in medium inoculated with cells. This was true for *C. crescentus* strains that develop pellicles (i.e., CB15) and strains that do not (i.e., NA1000) (Fig. 1C).

Biofilm development on solid surfaces is a robust area of study in part due to the development of powerful methods to visualize live cells attached to glass slides in flow chambers (35) and to quantify cells attached to surfaces by crystal violet staining (36). Neither of these techniques is directly applicable to the study of biofilm pellicle development at the air-liquid interface. As such, I developed a method to image *C. crescentus* cells from the pellicle. An intact plug of the pellicle could be captured by using the large end of a 1-ml pipet tip (Fig. 1D). This plug could be transferred to a glass slide and (i) covered with a coverslip for visualization by light microscopy (Fig. 1E) or (ii) allowed to adhere to the glass slide and stained with crystal violet (Fig. 2). I used these techniques to monitor pellicle development in static cultures starting at low density (optical density at 660 nm [OD_{660}] $\approx$ 0.005).

Phase-contrast imaging of plugs from the air-liquid interface revealed a rapid accumulation of cells at this boundary (Fig. 2). Within hours, cells formed an evenly dispersed monolayer at the liquid surface. Through time, monolayer density increased and eventually formed a cohesive network of cells. Cell density in the surface layer was distinctly greater than in the subsurface (bulk) medium (see Fig. S1 in the supplemental material), which suggested that cells partition to the air-liquid interface. By 24 h postinoculation, the surface monolayer had few, if any, gaps between cells. At this point, cells accumulated to a density at the surface of the liquid that was high enough to be visible as a film to the naked eye. In the monolayer stage, *C. crescentus* cells in plugs readily adsorbed to a glass surface and could be stained by crystal violet (Fig. 2). These plugs maintained well-formed edges (Fig. 1E and 2), and increased crystal violet staining of plugs was coincident with the increased density of the monolayer. The void left by removing a plug from the surface film was rapidly filled by the surrounding film at this stage, suggesting that an early-stage pellicle has fluid-like properties.

Between 24 and 48 h, a transition occurred from a monolayer to a multilayered structure that contained dense rosettes (Fig. 2). Simultaneously, the plug appeared less fluid and more cohesive; i.e., the removal of a plug from the pellicle at this stage left

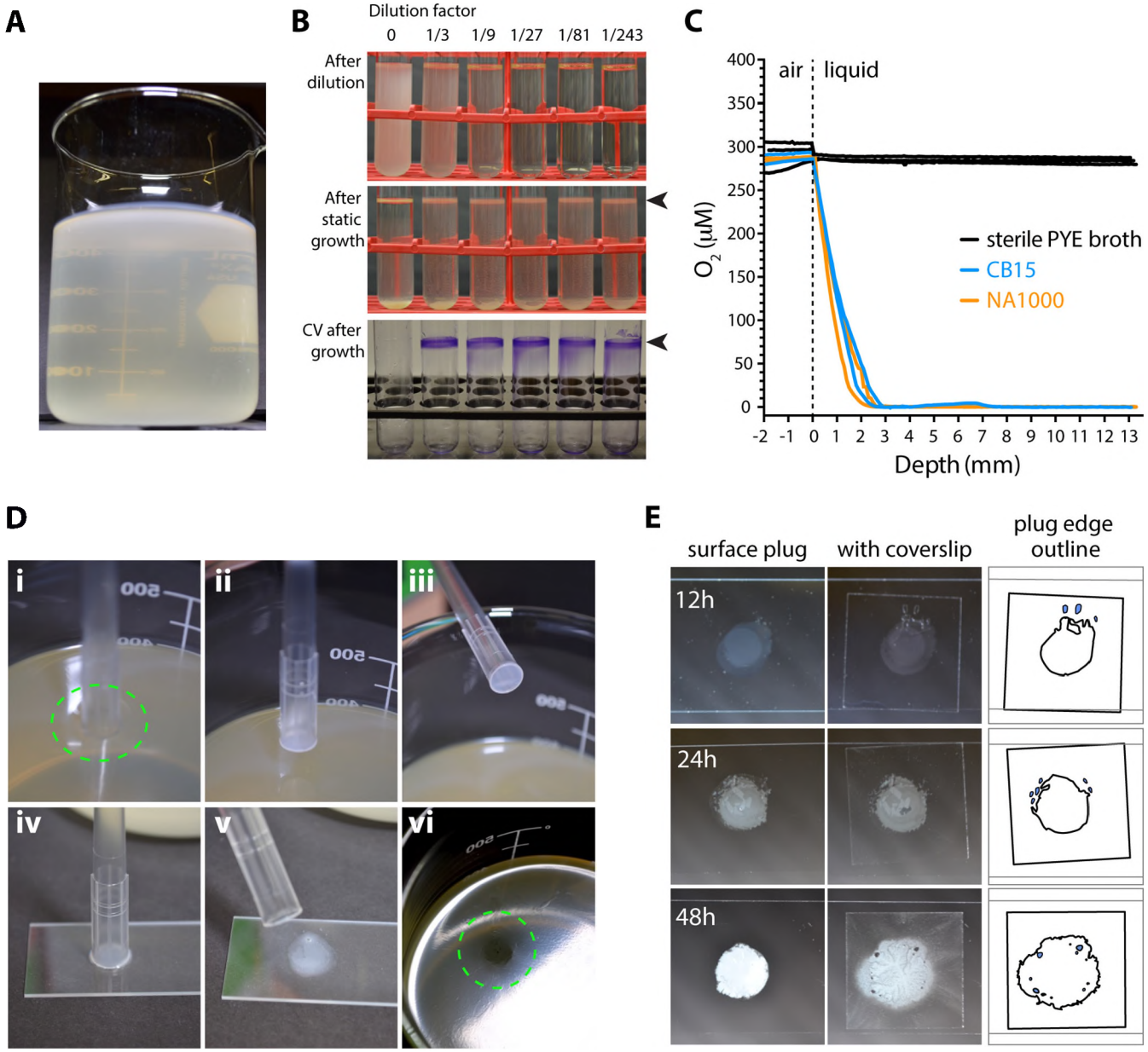

FIG 1 *Caulobacter crescentus* strain CB15 develops a pellicle at the air-liquid interface during static growth. (A) Wild-type *C. crescentus* CB15 culture grown at room temperature without mixing (i.e., static growth) for 3 days. Note the accumulation of cells in a pellicle at the air-liquid interface at the top of the beaker. (B) Pellicle development requires growth. (Top) A culture was grown to stationary phase under aerated conditions, transferred to a fresh tube (far left), and serially diluted with fresh medium (toward the right; dilution fractions are shown above each tube). (Middle) The same tubes are shown after incubation on the benchtop for 4 days. The arrowhead highlights colonization of the air-liquid interface in diluted cultures that grew postdilution but not in the undiluted culture. (Bottom) Crystal violet (CV) stain of cells attached to the tubes after cultures were washed away. The arrowhead highlights the position of the air-liquid interface. (C) The oxygen gradient is steep at the surfaces of unmixed cultures. Oxygen concentration as a function of depth from the surface (0 mm) was measured in beakers in which PYE medium was left sterile or inoculated with wild-type *C. crescentus* CB15 or wild-type *C. crescentus* NA1000 and incubated without mixing. Each trace represents an independent culture ($n = 2$). The limit of detection is 0.3 μM. (D) Method for sampling the pellicle. The large end of a sterile pipet tip is touched on the pellicle surface (i), lifted (ii, iii), and placed on a glass slide (iv, v). A pellicle scar (vi, circled) can be seen after the plug was removed from this 72-h culture. (E) Pellicle plugs were placed on glass slides (left column) and then covered with a coverslip (middle column). Outlines of the plugs under coverslips are on the right. The heavy line corresponds to the edges of the plugs. Stationary bubbles that formed upon placement of the coverslip are filled in blue. The time since inoculation is indicated for each sample.

a visible scar that was not filled by surrounding cells (Fig. 1D). Upon this transition to a multilayered rosetted structure, pellicle plugs no longer adhered to a glass slide. Instead, the plugs crumbled and washed away during staining. These thick multilayered pellicle structures were challenging to image by light microscopy. When flattened by a glass coverslip, the structures were compressed and/or dispersed; regions of the plug

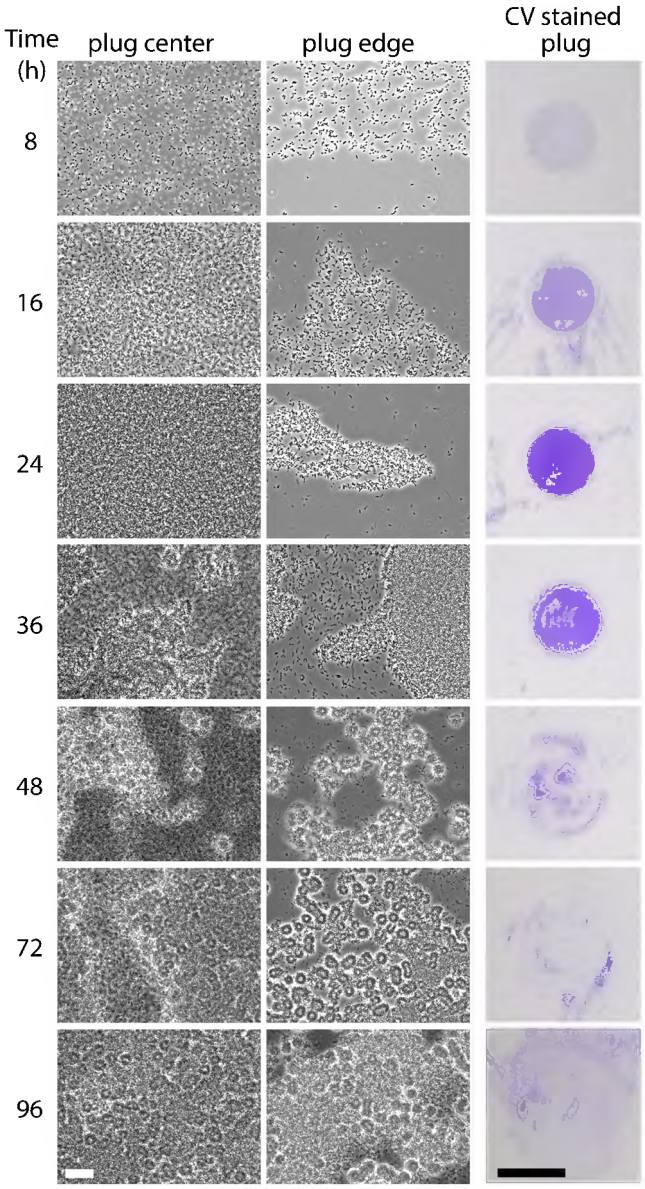

FIG 2 The pellicle develops from a homogeneous monolayer into a multilayered structure of dense rosettes. Surface plugs from a wild-type culture sampled periodically throughout static growth (the time after inoculation appears on the left) were evaluated by phase-contrast microscopy (left) and crystal violet (CV) staining (right). Two microscopy images are presented for each time point to capture the structure of cells in the center of the plug (left column) and also at the edges of the plug (right column; 8- to 36-h samples); cells disrupted from the multilayered plug structure were also imaged (right column; 48- to 96-h samples). Plug edges are outlined in Fig. 1E. White scale bar, 20 μm; black scale bar, 1 cm. This time course was repeated at least three times. Representative images from one experiment are presented.

that were less flattened by the coverslip appeared glassy when visualized by phase-contrast microscopy. In either case, it is clear that the mature pellicle consists of a dense network of connected rosettes. Connections between rosettes were often strong enough to withstand the forces of the fluid flow that was induced by placing a coverslip on the pellicle plug (Movie S1). Between 48 and 96 h, the pellicle became even thicker and more visible macroscopically. At some point after 96 h, pellicles typically crashed, sinking under their own weight, and settled in fragments at the bottom of the culture container.

Holdfasts are prominent in the pellicle. Many *Alphaproteobacteria*, including *C. crescentus*, form multicellular rosettes by adhering to each other through the polar

polysaccharide, or holdfast. Given the notable presence of rosettes in the pellicle, I sought to directly visualize the holdfast in the pellicle using fluorescent wheat germ agglutinin (fWGA), a lectin that binds to *N*-acetylglucosamine moieties in the holdfast polysaccharide. Typical holdfast staining protocols using fWGA involve pelleting and washing of the cells. To minimize disruptions to the pellicle structure during staining, I supplemented the medium with fWGA at the time of inoculation rather than at the time of staining after the pellicle was formed. I grew static cultures in the presence of 10, 1, or 0.2 μg/ml fWGA. The highest concentration delayed pellicle development (data not shown). Similarly, high concentrations (50 μg/ml) of WGA reduce holdfast adhesiveness to glass (37). In cultures with 1 or 0.2 μg/ml fWGA, pellicles developed similar to paired cultures without fWGA. I used 1 μg/ml of fWGA for these experiments, as signal was more intense than with 0.2 μg/ml.

In the early monolayer stages, nearly every cell was decorated with a holdfast at one cell pole (Fig. 3). Fluorescent puncta corresponding to the holdfast merged as the cell density in the monolayer increased. As a multilayered structure emerged (32 h), distinct patterns of holdfast staining were evident in the different layers. The top layer (i.e., closest to air) contained a dense array of holdfast puncta similar to that observed in the monolayer at 24 h. The lower layers of the plug contained a network of apparently interconnected rosettes whose cores stained prominently with fWGA (Fig. 3 [32 h] and Fig. 4). Bright fWGA puncta from rosette cores were observed in linear chains both in the center of intact pellicle plugs and in disrupted pellicle fragments (Fig. 4 and Fig. S2). As the pellicle matured, the lower layers became packed with rosettes. The cores of adjacent rosettes were connected in three dimensions in a manner that likely confers strength to the pellicle biofilm.

In fragments of dispersed pellicle film, the spatial relationship between the stained holdfast and the connected rosettes was more easily visualized (Fig. S2). Several types of structures were apparent. The tight focus of fWGA seen in radially symmetric rosettes is consistent with holdfasts adhering to each other at a single point. The cores of oblong rosettes are filled with many bright fWGA puncta and also a more diffuse fluorescent signal. This pattern suggests that the rosette center is filled with holdfast material. The cores of each holdfast in these rosettes do not bind a singular central focus but rather adhere in a mesh-like array.

The long axes of cells are perpendicular to the air-liquid boundary, with the holdfast at the interface. Imaging cells in surface layer plugs provides evidence that the holdfast directly positions *C. crescentus* at the air-liquid interface. Small, static bubbles occasionally form in the process of mounting a pellicle plug on a glass slide (Fig. 1E). These bubbles present the opportunity to observe cells at high magnification at an air-liquid interface. The long axis of cells at this interface was perpendicular to the boundary between the air bubble and liquid, with the holdfast positioned directly at the interface (Fig. 5). Moreover, when liquid flowed along stationary bubble edges, rafts of cells could be observed sliding along the boundary in the direction of flow (Movies S2 and S3). Cells in these rafts were perpendicular to the interface. The behavior of the cells attached to and moving along the bubble boundary was distinct from that of cells tumbling in the flow adjacent to the boundary.

Holdfast biosynthesis is required for pellicle formation. Based on my observation of (i) individual cells with holdfasts that occupy the air-liquid boundary and (ii) the presence of networks of rosettes in the pellicle, I tested whether the holdfast is necessary for pellicle formation. Strains lacking *hfsJ*, a gene required for holdfast synthesis (38), do not form macroscopically visible pellicles (Fig. 6). Not surprisingly, cells captured from the surface of Δ*hfsJ* cultures do not attach to glass slides, as evidenced by the lack of crystal violet staining (Fig. 7). At a microscopic scale, Δ*hfsJ* cells reach the surface microlayer as motile swarmer cells, but stalked and predivisional cells do not accumulate at the air-liquid interface (Fig. 8). I obtained similar results with strains lacking a functional *hfsA* holdfast synthesis gene.

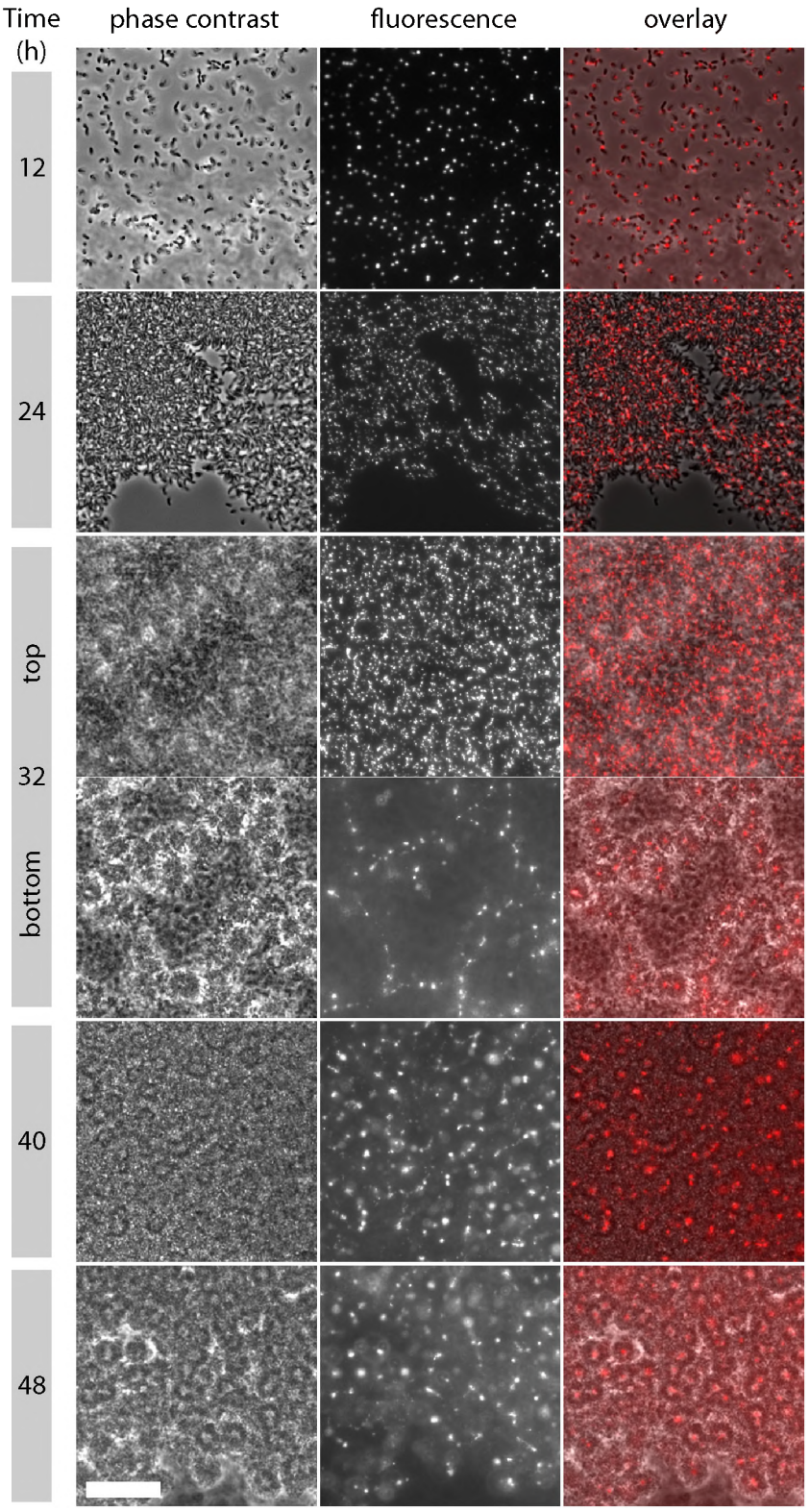

FIG 3 *In situ* fWGA-stained pellicle samples. Phase-contrast and fluorescence images of cells grown in the presence of 1 μg/ml fWGA sampled at time intervals after inoculation. During the transition from a monolayer to a multilayer structure, at 32 h, two focal planes of the same position in the pellicle plug are presented. These images correspond to the uppermost plane, where fWGA bound to individual cells is in focus, and the bottom plane just below the monolayer, where the centers of rosettes are in focus. At 40 and 48 h, focal planes from the middle of the film are shown. Scale bar, 20 μm. Representative images from one of several time courses are presented.

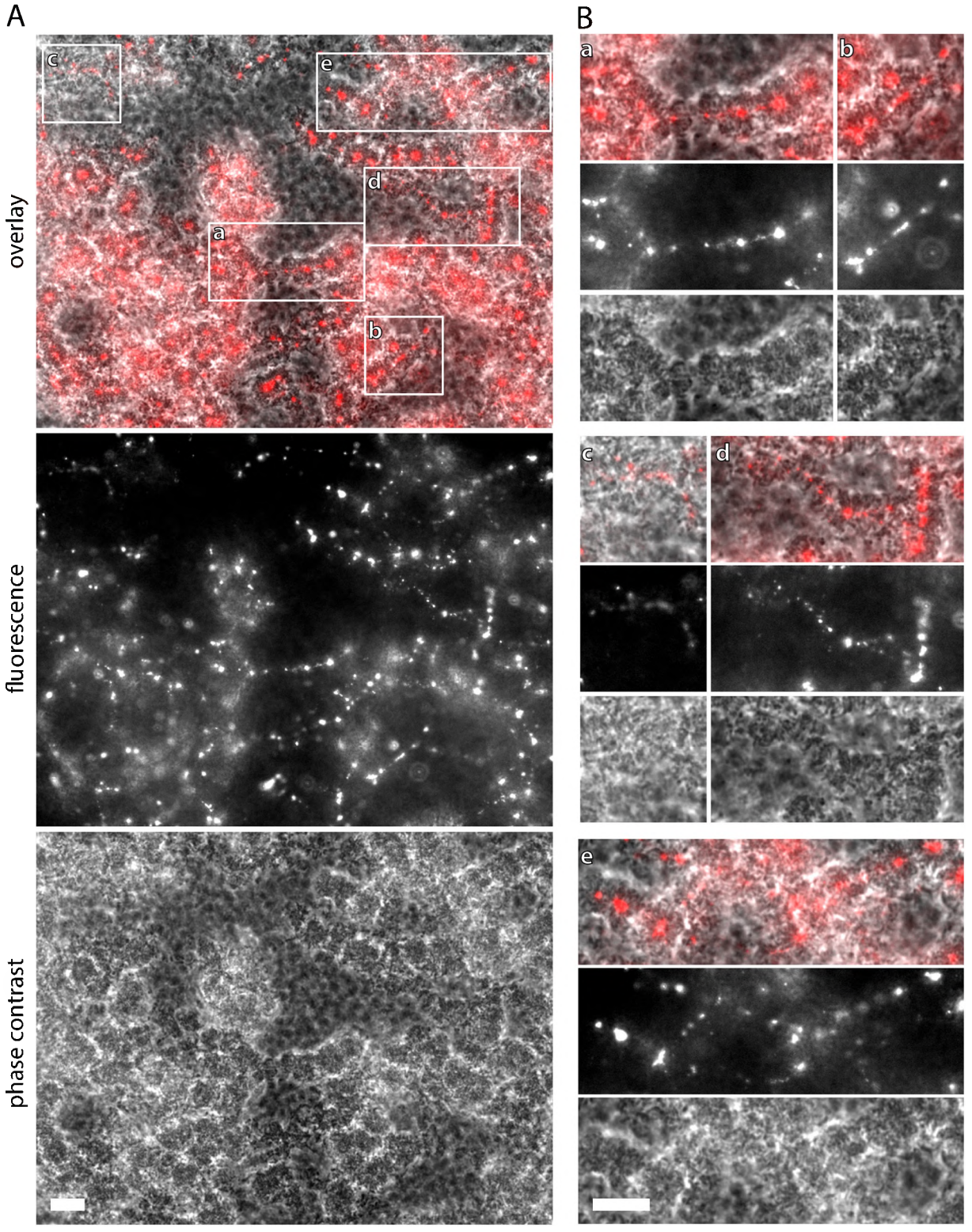

FIG 4 Linear arrays of rosettes in the center of an excised pellicle plug. (A) *In situ* fWGA-stained surface film harvested 40 h after inoculation. The focal plane is just below a monolayer. Overlay (top), fWGA-stained holdfast (middle) and phase-contrast (bottom) images from one field of view (137 μm by 104 μm) are shown. Note, some of the rosette chains extend beyond the focal plane. (B) Crops corresponding to the regions boxed in panel A. Scale bars, 10 μm.

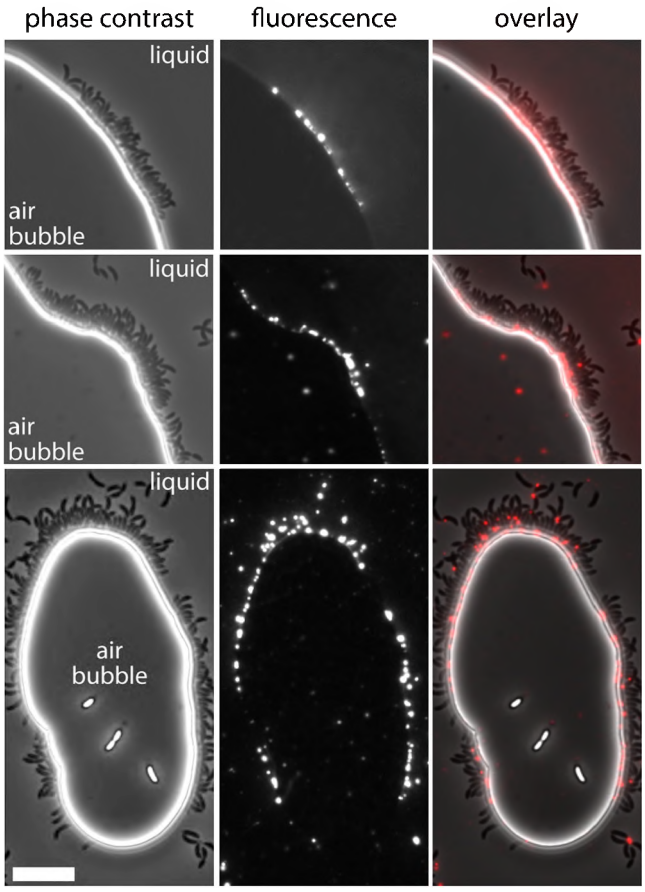

FIG 5 *C. crescentus* cells localized to the boundaries of air bubbles. Phase-contrast (left), fWGA-stained holdfast (middle) and overlay (right) micrographs from static cultures grown with fWGA, 8 to 12 h after inoculation. The interface between the air bubbles and the liquid medium is bright in phase-contrast images. The air and liquid sides of the boundary are indicated. Scale bar, 10 μm.

Holdfast biosynthesis is elevated in cells lacking *hfiA*, a negative regulator of holdfast biosynthesis (38). Pellicle development is accelerated in a Δ*hfiA* strain; these pellicles appear macroscopically thicker and leave plug scars at an earlier stage than the wild type (Fig. 6). Microscopically, the monolayer stage is similar to that of the wild type (Fig. 8), but the transition to a multilayered rosetted structure is more rapid, and the plugs

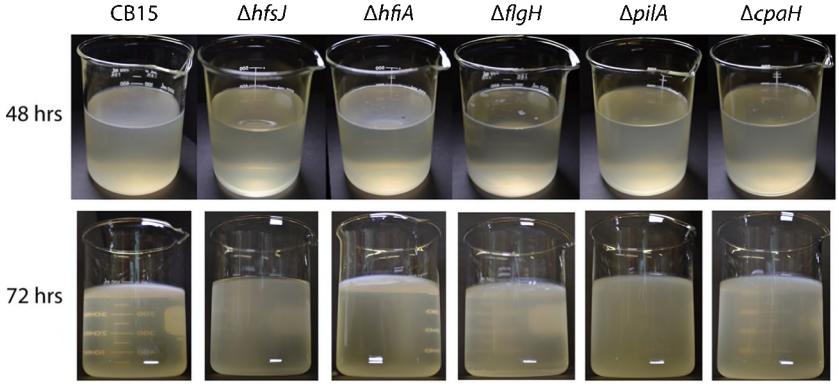

FIG 6 Macroscopic pellicles of polar appendage mutants. Static cultures of wild-type (CB15) and mutant strains 48 and 72 h after inoculation imaged from above and below, respectively. See the text for details on mutants. This experiment was repeated multiple times. The results of one representative experiment are shown.

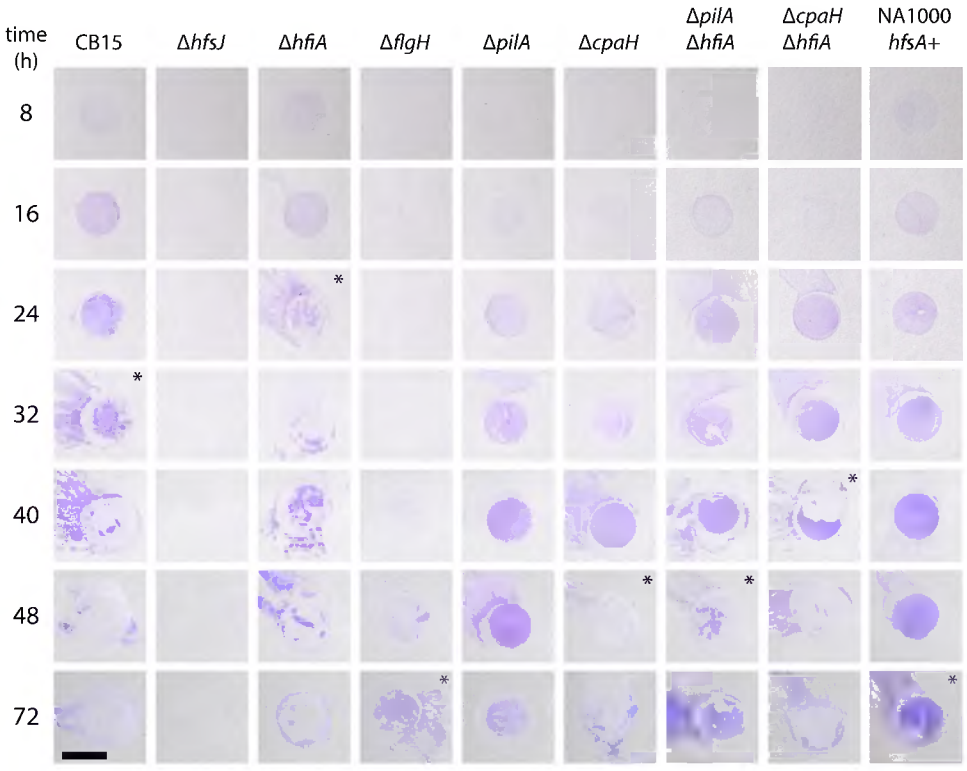

FIG 7 Crystal violet staining of pellicle plug samples. Pellicles of wild-type (CB15) and mutant strains sampled throughout development were evaluated by crystal violet staining. Note the three stages of pellicle development (CB15 times are indicated): adhesive monolayer (up to 24 h), crumbly transition phase (32 to 40 h), and nonadhesive film (48+ hours). For each genotype, the beginning of the crumbly phase is marked with an asterisk. Pellicles sampled are from the same experiment whose results are presented in Fig. 8 This experiment was repeated two additional times. Scale bar, 1 cm.

lose adherence to glass sooner (Fig. 7). Together these results indicate that the holdfast is essential for cells to accumulate at the air-liquid interface and for the development of the pellicle structure. Furthermore, enhancement of holdfast synthesis by deletion of *hfiA* promotes pellicle development.

Flagella and pili determine efficient pellicle development. Flagella and pili are important factors for the colonization of solid surfaces in *C. crescentus* (23, 26) and other species (39–41). Recently published data provide support for a complex interplay between the flagellum, type IV pili, and the control of holdfast development in *C. crescentus* (25, 31, 42–45). Given the clear role of the pilus and flagellum in attachment to solid surfaces and the regulatory connection between these structures and holdfast development, I tested the contribution of these appendages to *C. crescentus* pellicle development at the air-liquid interface. Specifically, I characterized pellicle development in a nonmotile strain lacking *flgH*, which encodes the outer membrane ring component of the flagellum. In addition, I assessed the role of the type IV pilus in pellicle development using a mutant lacking *pilA*, which encodes the pilus filament protein, and a mutant lacking *cpaH*, which encodes a transmembrane component required for type IV pilus assembly.

Nonmotile Δ*flgH* cells had dramatically delayed pellicle development. The pellicle that eventually emerged from this strain did not homogeneously cover the air-liquid interface but rather contained microcolony-like aggregates (Fig. 6). Δ*flgH* cells sampled at the air-liquid interface were primarily stalked or predivisional. At early time points, patches of cells attached to the coverslip, and small rosettes of 3 to 10 cells were abundant. Small rosettes were rarely observed in the surface samples from other strains. Larger rosettes and aggregates were also evident in Δ*flgH* pellicles (Fig. 8). With time, microcolonies consisting of dense mats of large rosettes emerged (Fig. 6 and 8,

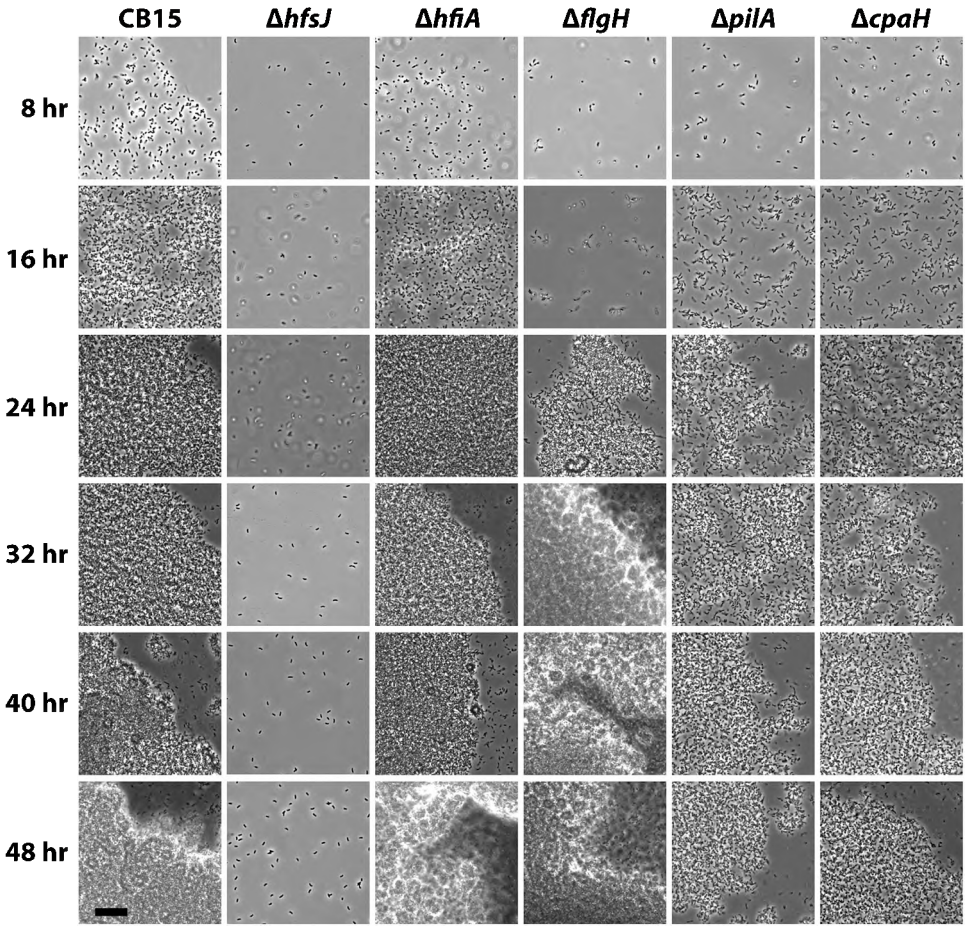

FIG 8 *C. crescentus* mutants lacking polar appendages exhibit defects in pellicle development. Phase-contrast micrographs of pellicle samples from wild-type (CB15) and mutant strains were taken at 8-h intervals. Scale bar, 20 μm. Representative images from one of three independent experiments are shown.

[40-h sample]). Eventually, the surface of the culture medium became covered with a film that did not adhere efficiently to glass and fragmented into large pieces (Fig. 7, 72 h). Though the nonmotile Δ*flgH* strain was unable to actively move to the air-liquid interface, the hyperholdfast phenotype of this strain (31, 44) seemed to enable capture of cells that arrived at the surface by chance. This resulted in cell accumulation and formation of the observed microcolonies at this boundary. I postulate that the inability of Δ*flgH* daughter cells to disperse, combined with premature holdfast development in this strain (44), promotes microcolony formation rather than a uniform distribution of cells at the air-liquid interface. These data support a model in which flagellar motility enables cells to efficiently reach the air-liquid interface but in which motility *per se* is not required for cells to colonize this microenvironment.

Both Δ*pilA* and Δ*cpaH* strains were defective in pellicle development. These pilus mutants are motile and capable of synthesizing holdfast. Both mutants accumulated at the air-liquid interface as monolayers similar to those of the wild type (Fig. 8). However, the density of these monolayers increased more slowly than that of the wild type. In addition, surface plugs from these mutant films retained the capacity to adhere to glass for a longer period (Fig. 7) and resisted scarring upon plug removal for an extended period of sampling. These observations are consistent with an extended monolayer phase. Even when dense monolayers formed, both mutants were defective in transitioning to a multilayered structure, as evidenced by microscopic images and crystal violet stains of surface plugs (Fig. 7 and 8).

It is notable that in a selection for mutants with surface attachment defects, these two mutants displayed distinct phenotypes; Δ*pilA* mutants had reduced surface attach-

ment, while Δ*cpaH* mutants displayed enhanced surface attachment owing to increased holdfast synthesis (31). Thus, in the context of attachment to solid surfaces, increased holdfast synthesis can outweigh defects from the loss of pili. In pellicle development, on the other hand, the defects in these two classes of pilus mutants were nearly the same. The primary difference was that the Δ*cpaH* mutant transitioned to a nonadherent, crumbly film sooner than the Δ*pilA* mutant, as might be expected for a strain with elevated holdfast synthesis (Fig. 7). Even though Δ*cpaH* mutant transitioned to a crumbly structure sooner than the Δ*pilA* mutant, its crumbly structure was still significantly delayed compared to that of the wild type. In addition, microcolonies were often observed in Δ*cpaH* surface films but were smaller and less pronounced than in the Δ*flgH* surface films (Fig. 6).

Finally, I examined pellicle development in Δ*pilA* and Δ*cpaH* mutants that also carried an in-frame deletion of *hfiA* in order to test whether elevated holdfast production could overcome the defects associated with the loss of pili. The Δ*pilA* Δ*hfiA* and Δ*cpaH* Δ*hfiA* double mutant strains transitioned to a crumbly, nonadherent film sooner than their Δ*pilA* and Δ*cpaH* counterparts. However, both double mutant strains were still delayed compared to the Δ*hfiA* single mutant and were not restored to wild-type pellicle development (Fig. 7). Together, these data indicate that pili are not required for *C. crescentus* to colonize the air liquid interface, but these appendages do contribute to the formation of a dense, robust pellicle. Moreover, these data indicate that elevated holdfast production promotes pellicle development but is not sufficient to fully compensate for the loss of pili.

Pellicle architecture is influenced by an MGE. NA1000 is a standard laboratory strain that is almost completely isogenic with CB15 (46) and is used to produce synchronized populations of *C. crescentus* for cell cycle studies (47). The synthesis of an extracellular polysaccharide (EPS) on the surfaces of stalked cells, but not of newborn swarmer cells, enables isolation of NA1000 swarmer cells by centrifugation in Percoll (48). Genes required for the synthesis of this cell cycle-regulated EPS are carried by a mobile genetic element (MGE) that is present in the NA1000 genome but missing from CB15 (46). In addition, NA1000 is defective in holdfast formation owing to a frameshift mutation in *hfsA* (46).

NA1000 did not develop pellicles under static growth conditions. Restoration of *hfsA* to a functional (nonframeshifted) allele was sufficient to enable pellicle formation in this background (Fig. 9A). However, NA1000 *hfsA*$^+$ pellicles were qualitatively different from CB15 pellicles in many respects. NA1000 *hfsA*$^+$ pellicles were more fluid; i.e., voids from pellicle plugs quickly filled in rather than leaving scars. In addition, plugs from mature NA1000 *hfsA*$^+$ pellicles did not crumble like CB15 plugs (Fig. 7). At a microscopic level, I observed more space between NA1000 *hfsA*$^+$ cells from the center of the film and in dispersed rosettes than between CB15 cells. NA1000 *hfsA*$^+$ rosettes were less tightly packed and more interwoven than CB15 rosettes (Fig. 9B). In short, even though restoration of the *hfsA* frameshift in NA1000 restores holdfast development and pellicle formation, there are significant phenotypic differences in cell packing and pellicle architecture between *C. crescentus* strains NA1000 and CB15.

Based on these observations, I reasoned that the NA1000-specific EPS (synthesized by gene products of the MGE) may be responsible for pellicle differences between CB15 and NA1000. To test this hypothesis, I grew static cultures of an NA1000 isolate from which the MGE had spontaneously excised (NA1000 ΔMGE) (46) and an isogenic strain in which I restored the null frameshift mutation in *hfsA* (NA1000 ΔMGE *hfsA*$^+$). As expected, the NA1000 ΔMGE strain with the frameshifted *hfsA* allele did not accumulate at the air-liquid interface, and restoration of *hfsA* enabled pellicle development (Fig. 9A). Loss of the MGE, and thus cell cycle-regulated EPS, resulted in a pellicle architecture that more closely resembled CB15's, with closer cell packing and more compact rosettes (Fig. 9B). In addition, the enhanced buoyancy conferred by the MGE was apparent when culture medium below the surface was observed. CB15 and NA1000 ΔMGE *hfsA*$^+$ cells not trapped at the air interface tend to settle to the bottom. NA1000 *hfsA*$^+$ cells were

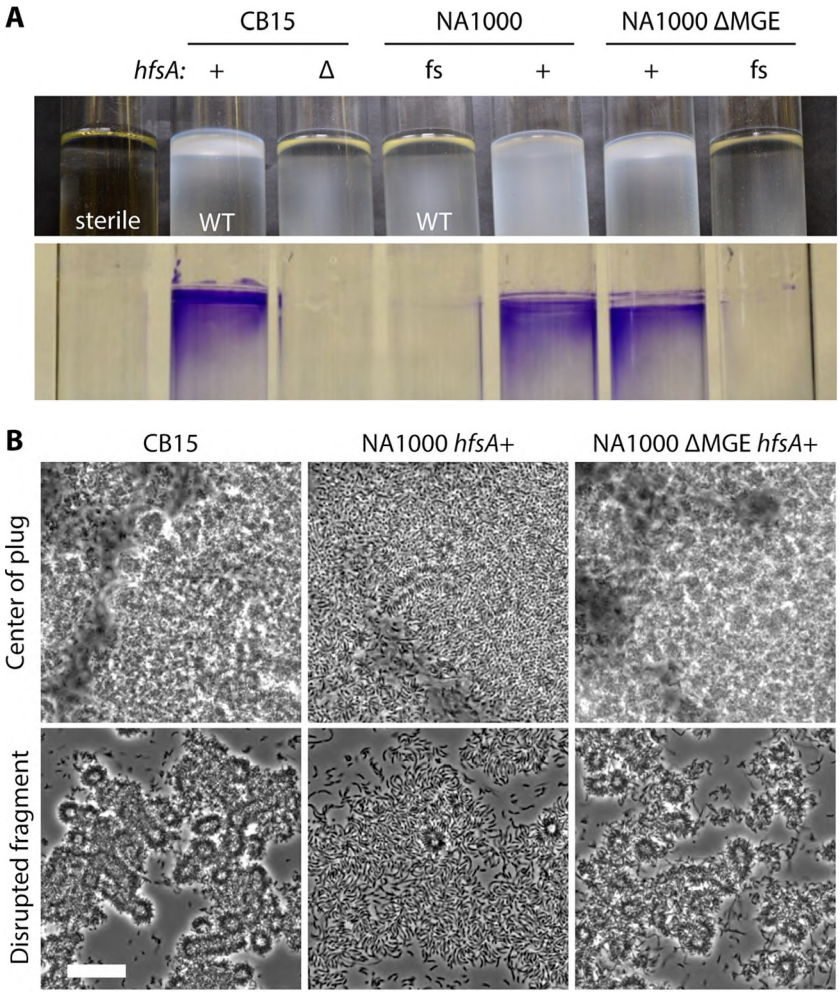

FIG 9 Pellicle structures of NA1000 strains differ from those of CB15. (A) Pellicles of cultures grown statically for 3 days are pictured (top). After growth, the tubes were stained with crystal violet to highlight cells adhered to the glass at the surfaces of the cultures (bottom). Genotypes of strains are indicated above the tubes. Strains that differ only at the *hfsA* locus are paired, and the *hfsA* allele is indicated as the functional CB15 allele (+), the null allele (Δ), or the frameshifted NA1000 allele (fs). See the text for details about the mobile genetic element (MGE). A tube with sterile medium (left) demonstrates the characteristics of an uncolonized meniscus, similar to what is seen at the surface of medium colonized with strains lacking a functional *hfsA* allele. The whole surface of the culture is opaque when a pellicle film is present. WT, wild type. (B) Phase-contrast micrographs of pellicle samples from CB15, NA1000 *hfsA*$^+$, and NA1000 ΔMGE *hfsA*$^+$ pellicles collected 48 h after inoculation. The center of the plug (top) and rosettes disrupted from the film (bottom) were imaged. Scale bar, 20 μm.

more evenly distributed throughout the depth of the culture (Fig. 9A), presumably owing to the cell cycle-regulated EPS present on the nonmotile stalked cells (46, 48).

It is worth noting that several phenotypic differences between CB15 and NA1000 were not determined by the presence/absence of the MGE. Specifically, NA1000-derived cells were notably larger than CB15 cells and more prone to filamentation in the pellicle context, regardless of the MGE. The genetic polymorphisms responsible for these phenotypic differences have not been determined.

The MGE present in NA1000 strains accounts for the major differences in cell packing and pellicle architecture between CB15 and NA1000. This observation supports a model in which the modulation of secreted polysaccharides has profound effects on cell-to-cell interactions and possibly on cell-to-interface interactions at boundaries. These strain differences should be considered as investigators look toward future studies of *C. crescentus* attachment behavior and biofilm development.

***Caulobacter* accumulates at the air-liquid interface in dilute media.** The thick pellicle films observed in static culture in PYE medium involve high densities of cells;

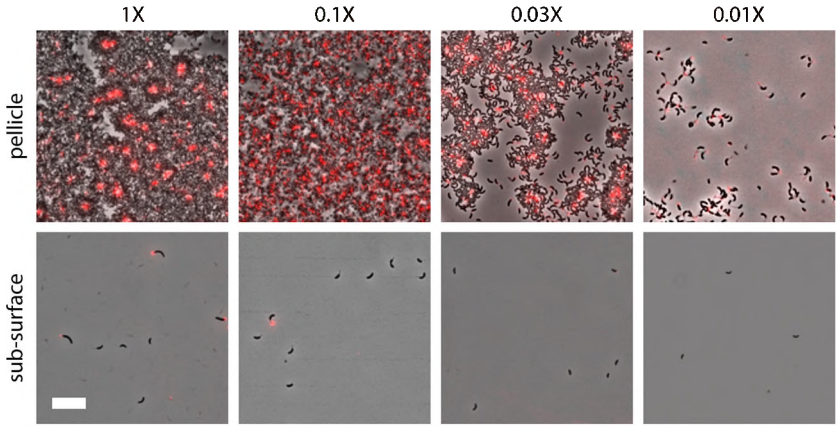

FIG 10 Cells partition to the air-liquid boundary in dilute complex medium. Surface and subsurface samples of *C. crescentus* CB15 were cultured in increasingly dilute PYE medium. Dilution factors from the standard lab recipe (see Materials and Methods) are indicated at the top. Cultures were grown statically with fWGA to stain the holdfast for 2.5 days. Samples were imaged using phase-contrast and fluorescence imaging, and an overlay is presented for each condition. Scale bar, 10 μm.

PYE can support growth to 10^8 to 10^9 CFU/ml. I wondered whether *C. crescentus* could form a pellicle film in a more nutrient-limited environment, i.e., in a medium that did not support such high cell density. To address this question, I used a series of increasingly dilute complex media rather than a mineral defined M2-based medium for two main reasons: (i) standard M2-based media support dense cell growth (i.e., are not growth limiting) and (ii) there is evidence that complex media better reflect the complex suite of nutrients encountered by *Caulobacter* in natural ecosystems (34). While progressive dilution of a complex medium certainly reduced culture density (and cell size), a thick pellicle was observed in 0.1× PYE, large rosettes accumulated at the surface of 0.03× PYE, and small clusters of 2 to 4 cell rosettes formed on the surfaces of cultures grown in 0.01× PYE (Fig. 10). The density of cells in the pellicle was proportional to the carrying capacity of the growth medium. Importantly, under all these conditions, the distribution of cells was strongly biased toward accumulation at the air interface (Fig. 10). Thus, even in highly diluted medium, *C. crescentus* partitions to the air-liquid interface.

DISCUSSION

Alphaproteobacterial model for biofilm development at the air-liquid boundary. Molecular factors that contribute to colonization of solid surfaces in both environmental and host-microbe contexts are well understood for many bacterial species. While biofilms at the air-liquid boundary have been studied, they have received less attention than other biofilms, and our understanding of the molecular determinants of biofilm development at such interfaces is less well developed. Data presented in this study define distinct stages of pellicle development in *C. crescentus*, a model *Alphaproteobacterium*. The *C. crescentus* pellicle does not initiate at the solid edges of the air-liquid interface but rather develops uniformly across the entire liquid surface. Initially, individual cells accumulate at this boundary as an evenly dispersed monolayer of individual cells trapped at the interface. When the monolayer becomes sufficiently dense, rosettes accumulate beneath the monolayer and eventually form a multilayered pellicle structure comprised primarily of large dense rosettes (Fig. 2). These stages are reminiscent of biofilm development on solid substrates, in which surfaces are often initially colonized with a monolayer of cells before more-complex three-dimensional structures form. I propose that *C. crescentus* colonization and pellicle formation at the air-liquid boundary constitute an experimentally tractable model for the study of biofilm development in an *Alphaproteobacterium*.

While it is known that bacteria will form monolayers at air-liquid interfaces in natural settings, and I observed partitioning of *C. crescentus* to the air interface in 100-fold-

diluted PYE (Fig. 10), the ecological relevance of the thick three-dimensional structures that I observed in later stages of *C. crescentus* pellicle development is not clear. Poindexter describes individual prosthecate cells but not rosettes in environmental samples; rosettes were evident only in her pure cultures (20). Similarly, in surface samples collected directly from a freshwater pond, Fuerst et al. described prosthecate cells but did not note rosettes in this study (49). I am not aware of any descriptions of *Caulobacter*, or other rosette-forming *Alphaproteobacteria*, producing rosettes outside the laboratory. One expects that rosettes and three-dimensional *Caulobacter* pellicles/films should occur only in environments with sufficient nutrients to support high cell densities. That said, recent metagenomic analyses challenge the historical view that *Caulobacter* species are oligotrophs that exclusively inhabit dilute aquatic environments (18). *Caulobacter* species are broadly distributed in soil and aquatic environments and are most prevalent in systems with abundant decaying plant matter, which are not associated with nutrient limitation (18). Thus, it may be the case that *Caulobacter* spp. form thick pellicles in static aquatic systems rich in decaying plant material. Regardless, the holdfast clearly enables exploitation of the air-liquid interface, even at low cell density (Fig. 10).

Multiple polar appendages contribute to pellicle development. *C. crescentus* swarmer cells are born with a single flagellum and multiple pili that decorate the old cell pole, and they are preloaded with the machinery to elaborate a holdfast at this same pole (20, 23, 24). Development of these surface appendages is intimately tied to the cell cycle and is central to the lifestyle and ecology of *Caulobacter* species. Specifically, the flagellum confers motility and enables swarmer cells to disperse, while the flagellum and the pili together contribute to reversible attachment during colonization of solid surfaces. When deployed, the holdfast confers irreversible attachment to solid surfaces (20, 23, 26, 37, 50). In colonization of the air-liquid interface, each of these appendages also plays important roles. Cells lacking a functional flagellum are unable to efficiently reach the interface and, instead, arrive there only by chance. Cells unable to synthesize the holdfast reach the liquid surface as motile swarmers but do not remain after differentiation into nonmotile stalked cells. Thus, holdfast mutants do not accumulate at the surface and cannot form a dense pellicle film. Finally, cells lacking pili efficiently reach the air-liquid interface and accumulate to high densities but exhibit developmental delays. A synthesis and discussion of published data on the *C. crescentus* flagellum, pili, and holdfast in the context of my results follow.

Flagellum. The requirement that *C. crescentus* be motile to efficiently reach the air-liquid interface (Fig. 6 and 8) is not particularly surprising. Genes involved in aerotaxis and motility are known determinants of pellicle formation in other aerobes (e.g., see references 16 and 51 to 54). *C. crescentus* is capable of aerotaxis (55), though the requirement for aerotaxis *per se* in *C. crescentus* pellicle formation remains undefined, as the sensors are unknown. While static *C. crescentus* cultures have a steep oxygen gradient at the air interface (Fig. 1C), nonmotile or nonadhesive *C. crescentus* mutants can still grow to high density in static culture. This is consistent with a tolerance of this species for microoxic conditions (56).

While motility is required for cells to efficiently reach the surface, I have shown that it is not explicitly required for accumulation at the surface. Δ*flgH* mutants, which lack a flagellum, colonize the air-liquid interface, albeit less inefficiently than wild type (Fig. 6 and 8). It is known that the loss of some flagellar genes, including *flgH* and *flgE*, results in a hyperholdfast phenotype (31, 44). In the context of pellicle development, the observed microcolonies of rosettes in the Δ*flgH* strain suggests that its hyperholdfast phenotype can overcome the motility defect of this strain.

Holdfast. Data presented in this study provide evidence that the holdfast can function to trap cells at the air-liquid interface. Mutants defective in holdfast synthesis cannot partition to the surface layer (Fig. 6 and 8). Inspection of bubble surfaces formed when samples were mounted for microscopy revealed that cells positioned themselves perpendicular to the bubble boundary, with the holdfast pole occupying the air-liquid

interface (Fig. 5). I infer that the holdfast allows polar attachment of replicative stalked cells to air-liquid interfaces as it does to solid surfaces. The observations reported here are reminiscent of an earlier report that the alphaproteobacterium *Hyphomicrobium vulgaris* stands perpendicular to air-liquid, liquid-liquid, and solid-liquid boundaries, with the replicative pole at the interface (57).

How might the holdfast enable cells to remain at this interface, and what can be inferred about the nature of the holdfast material from these observations? The microlayer between the bulk liquid and the air represents a unique physiochemical environment. Hydrophobic and amphipathic molecules partition to this boundary (1, 2, 7, 10). Surface hydrophobicity is an important feature of bacteria that colonize the air-liquid interface (58). Though the exact chemical nature of the holdfast is not known, the fact that it apparently partitions to this zone implies that it has hydrophobic, or at least amphipathic, properties. A similar conclusion was reached regarding the unipolar polysaccharides secreted by *H. vulgaris* and the unrelated sphingobacterium *Flexibacter aurantiacus* (57).

The air-liquid interface of complex aqueous broth is more viscous than the bulk solution owing to polymers adsorbed at this surface (7, 8, 15, 59). Increased surface viscosity is responsible for trapping motile swarmer cells at the air-liquid interface (59) and may also trap the holdfast, which itself is secreted as an amorphous viscous liquid (60). In sum, the holdfast can apparently function to partition nonmotile replicative cells to the air-liquid interface. This function is likely important for an aerobe that is motile (and aerotactic) only in the nonreplicative swarmer phase of its life cycle.

How then do rosettes, in which the holdfast is buried in the interior of a cluster of cells, partition to the air-liquid boundary? The answer to this question is not clear from the data presented in this paper. One possibility is that the holdfast polymer excludes water from the rosette core to an extent that it reduces the density of the collective aggregate. More extensive biophysical characterization of rosettes will lead to a better understanding of the role of these structures in partitioning to the air-liquid interface and in pellicle development.

Pilus. Type IV pili are not required for cells to reach or adsorb to the air-liquid interface (Fig. 8). However, cells lacking pili inefficiently reach high densities at the interface and are extremely delayed in the transition to a multilayered pellicle structure, even when holdfast production is elevated. I envision two nonexclusive explanations for this result: (i) pili are important factors mediating cell-cell interactions and facilitate the coalescence of cells during rosette formation and (ii) pili constitute a matrix component that confers strength and rigidity to the pellicle. Pili can extend up to 4 μm in length (61) and physically retract (43). Pilus interactions between neighboring cells should increase load during pilus retraction, thereby stimulating holdfast production (43) while simultaneously bringing holdfast-bearing cell poles in closer proximity. In this way, pili may organize cells and promote rosette development. This model is similar to that described for *Neisseria gonorrhoeae*, where pilus interactions and pilus motor activity promote dense packing of cells (62–64). Electron micrographs of rosettes of the closely related species *Asticcacaulis biprosthecium* reveal a network of pili surrounded by the holdfast at the junction between poles (65). These snapshots lead one to speculate that pilus retraction brought these cell poles together. The *A. biprosthecium* micrographs, combined with the results described here, inform the hypothesis that pili confer structural support to reinforce holdfast-mediated interactions between cells.

I observed, although it was difficult to capture by standard light microscopy, that assemblies of cells were less organized at the air-liquid interface in both pilus-null strains (Δ*pilA* and Δ*cpaH* mutants). In these mutants, it was often difficult to assess whether cells were arranged in a rosette (i.e., attached at the distal end of the stalked poles) or simply in an unordered clump of nonspecifically adherent cells. This qualitative conclusion held true in blind analyses of pellicle plugs where the strain genotype was not known to me. My observations support a role for the pilus in organizing and promoting cell-cell interactions. In many species, type IV pili mediate motility; however,

in *Caulobacter*, the primary role of these appendages seems to be attachment to surfaces (26, 43, 66, 67). As an extension, I propose that *C. crescentus* pili facilitate cell-cell attachments in the context of the pellicle. The role of type IV pili in cell-cell interactions and robust pellicle formation merits further study.

Finally, I note that the role of pili in mediating attachment is context dependent. In a pellicle, mutants lacking the pilus filament (Δ*pilA* mutant) or a component of the pilus assembly machine (Δ*cpaH* mutant) exhibit similar phenotypes. In the context of attachment to cheesecloth or polystyrene, the Δ*pilA* mutant has attenuated surface attachment, while a Δ*cpaH* strain exhibits hyperattachment (31). In shaken broth, deletion of *cpaH* increases the fraction of cells with a holdfast, while deletion of *pilA* does not affect the probability of holdfast development (31). On an agarose pad, cells lacking *pilA* exhibit delayed holdfast development (44). Collectively, these results indicate that physical/environmental constraints likely influence the relative importance of the pilus function *per se* and pilus regulation of holdfast development upon attachment.

On the formation of cell chains and the putative threads that connect them. Fluorescence imaging of pellicles reveals rosette cores as well as looser assemblies of cells that appear to be connected in linear arrays (Fig. 3 and 4; also see Fig. S2 in the supplemental material). Properties of the rosette exterior may facilitate connections between rosettes, but rosette surface connections alone should be nondirectional and result in randomly organized aggregations of rosettes. The linear nature of the connections suggests the possibility of a thread-like structure that does not stain with fWGA but to which holdfast-bearing cells can attach (Fig. 3 and 4 and Fig. S2). What, then, might be this material to which holdfasts adhere and that may mediate longer-range interactions in a pellicle? The length of the connections suggests a polymeric molecule (polysaccharide, DNA, or a protein fiber). This putative material does not bind WGA, suggesting that it is not holdfast polysaccharide, unless the cell produces a modified form lacking *N*-acetylglucosamine. In the pellicle context, *C. crescentus* may synthesize a previously uncharacterized extracellular polysaccharide. For example, *Agrobacterium* elaborates a polar adhesin and also synthesizes extracellular cellulose fibrils that aid in cell aggregations and attachment to plant cells (68, 69). It is also possible that these threads are DNA. This molecule is a well-established component of the biofilm matrix of other bacteria (17). DNA associates with the outer layers of the *C. crescentus* holdfast and similarly is observed adjacent to the holdfast polysaccharide in rosette cores (33). In other work, DNA released during cell death was demonstrated to bind to holdfast and inhibit attachment (70). This suggests a model in which DNA associates with the holdfast polysaccharide and at sufficiently high concentrations masks the adhesin, as occurs with high concentrations of WGA (37). Finally, polymers of proteins such as pili or flagella may conceivably facilitate long-range interactions. Pili are observed in rosettes of *Asticcacaulis* (65), and cells lacking PilA are defective in the development of these multicellular structures in the pellicle (Fig. 8). However, this filament is typically retracted into the cell, and single pilus filaments are too short to facilitate interactions of the length scale that I observed. Flagellar polymers, on the other hand, are shed into the medium (71), though they are occasionally observed still attached at the end of a stalk extension (20). It may be the case that overlapping mixtures of these filamentous materials produce these "threads." Future work will be necessary to identify this putative component of the *Caulobacter* pellicle biofilm.

Distribution and ecological importance of the holdfast in *Alphaproteobacteria*. Synthesis of a holdfast-like adhesin at one cell pole is a broadly conserved trait in *Alphaproteobacteria*. Examples of species that secrete polar adhesins or form polar rosette aggregates have been described in almost every alphaproteobacterial order, including *Rhizobiales* (72–81), *Caulobacterales* (20, 37, 65, 82–84), *Rhodobacterales* (85–90), and *Sphingomonadales* (91–93). Exceptions are *Rhodospirillales* and *Rickettsiales*, which are at the base of the alphaproteobacterial tree (94). The ensemble of holdfast synthesis genes (29, 30, 72, 79, 82, 88, 95) and chemical compositions of the holdfast polysaccharides (37) vary between species and families, which may reflect chemical differences in the niches that particular species colonize.

TABLE 1 Strains used in this work

Strain	Genotype	Source or reference
FC19	*C. crescentus* CB15	20, 96
FC20	*C. crescentus* NA1000	46
FC1974	CB15 Δ*hfsJ*	38
FC1356	CB15 Δ*hfiA*	38
FC1266	CB15 Δ*flgH*	31
FC1265	CB15 Δ*pilA*	31
FC3013	CB15 Δ*cpaH*	31
FC3084	CB15 Δ*pilA* Δ*hfiA*	31
FC3083	CB15 Δ*cpaH* Δ*hfiA*	31
FC767	CB15 Δ*hfsA*	46
FC764	NA1000 *hfsA*$^+$	46
FC766	NA1000 ΔMGE	46
FC3366	NA1000 ΔMGE *hfsA*$^+$	This work

For many *Alphaproteobacteria*, the advantage of a polar adhesin for attachment to surfaces is obvious: *Agrobacterium* and *Rhizobium* adhere to plant roots during infection and symbiosis, respectively, and *Roseobacter* interacts with algae in a symbiosis and to submerged abiotic surfaces that are coated by conditioning films. I propose that attachment/partitioning to air-liquid interfaces is a general function of holdfast-like polar polysaccharides in some species. For example, *Phaeobacter* strain 27-4 and other *Roseobacter* spp. form interlocking rosettes at the air-liquid interface in static cultures (86, 87). In biofilm assays, *Caulobacter* and *Agrobacterium* attach most robustly at the air–solid-liquid interface, and this attachment requires a polar adhesin (e.g., references 44 and 95 and Fig. 1B). For *Alphaproteobacteria* that are aerobic heterotrophs, the advantage of a cellular mechanism to exploit elevated nutrients and oxygen at the air-liquid interface is clear. The holdfast can provide this function.

MATERIALS AND METHODS

Growth conditions. The *C. crescentus* strains used in this study are derived from the CB15 wild-type parent unless otherwise noted; see Table 1. All strains were cultured in peptone-yeast extract (PYE) broth containing 0.2% peptone, 0.1% yeast extract, 1 mM $MgSO_4$, 0.5 mM $CaCl_2$. PYE was solidified with 1.5% agar for propagation of strains. Strains detailed in Table 1 were struck from −80°C glycerol stocks onto PYE agar and grown at 30°C or room temperature (20 to 24°C) until colonies appeared after 2 to 3 days. For static growth experiments, starter cultures (2 to 10 ml) were inoculated from colonies and grown with aeration overnight at 30°C. Starter cultures were diluted to an optical density at 660 nm (OD_{660}) of approximately 0.005 and grown without shaking on the benchtop at room temperature (20 to 23°C). For experiments requiring repeated sampling through time, I grew cultures with larger surface areas to avoid resampling from the same position. In such experiments, 400 ml of culture was grown in 600-ml Pyrex beakers (9-cm diameter) covered in foil to prevent contamination. In experiments involving only macroscopic inspection of pellicle development, static cultures were inoculated at similar starting densities and grown in test tubes. In preparation of dilute complex medium, the peptone and yeast extract were diluted accordingly from the 1× concentrations of 0.2% and 0.1%, wt/vol, respectively. The $MgSO_4$ and $CaCl_2$ concentrations were held constant at 1 and 0.5 mM, respectively.

Strain construction. Most of the strains used in this study were previously constructed and reported (Table 1). To restore the frameshifted *hfsA* allele on the chromosome of the NA1000 ΔMGE strain, I used a standard two-step recombination approach. The pNPTS138-based allele replacement plasmid carrying the *hfsA*$^+$ allele was previously reported, along with methods for using this plasmid (46).

Sampling from the surface. To capture minimally disturbed cells from the air-liquid interface, I placed the large end of a 1-ml pipet tip on the surface of the static culture. Lifting the tip removed the corresponding segment of the surface layer as a plug (Fig. 1D). I placed the end of the tip carrying the plug sample on a glass slide. I gently applied air pressure to the opposite small end of the tip as I lifted the tip from the slide to ensure complete sample transfer.

Sampling from the subsurface. Pipet tips that pass through the pellicle film become coated with film and transfer these cells to anything that directly touches the outside the tip. To minimize capture of the pellicle when sampling the subsurface, I submerged a tip 3 to 4 cm below the liquid surface, expelled air through the tip to blow out any liquid that may have entered the tip and then aspirated several hundred microliters of culture into the tip. After removal of the tip, the culture was rapidly expelled into a sterile tube without making contact between the tip and the tube. If the culture was slowly expelled, the liquid would creep up the side of the tip and capture cells from the pellicle film. Several microliters of the subsurface sample were placed on a glass slide and covered with a coverslip for microscopic imaging.

Microscopy. Surface layer plugs placed on glass slides were covered with glass coverslips (Fig. 1E) and imaged using phase-contrast microscopy with an HCX PL APO 63×/1.4-numerical-aperture Ph3 oil

objective on a Leica DM5000 upright microscope. Images were captured with a Hamamatsu Orca-ER digital camera using Leica Application Suite X software.

Fluorescent staining of the holdfast. For staining of the holdfast *in situ*, cultures were supplemented with 1 μg/ml fluorescent wheat germ agglutinin conjugated to Alexa Fluor 594 (Thermo Fisher) (fWGA) at the time of inoculation. These static cultures were grown under a cardboard box to minimize photobleaching. Samples were collected as described above and imaged in the phase-contrast and fluorescence imaging modes using Chroma filter set 41043.

Crystal violet staining of pellicle plugs. Surface plugs were placed on glass slides and allowed to stand for 2 to 4 min. After slides were rinsed under flowing tap water, a slide was covered with a 0.01% crystal violet solution in water (approximately 1 to 2 ml to cover the slide). After 3 to 5 min of incubation, the slide was rinsed again and allowed to dry. Stained plugs were photographed with a 35-mm Nikon digital camera.

Oxygen profiling. Oxygen concentrations were measured with a Unisense Field Multimeter 7614 equipped with a motor-controlled micromanipulator and a Clark-type oxygen microelectrode (OX-25; 20- to 30-μm probe diameter; Unisense). Two point calibrations were performed with air-saturated deionized H_2O ($[O_2] \approx 283$ μM) and a solution of 0.1 M sodium hydroxide, 0.1 M sodium ascorbate (anoxic standard). Calibrations were checked throughout the experiments. Oxygen measurements were performed in 100-μm steps downward, starting at the top of the culture. The sensor limit of detection is 0.3 μM O_2. Profiles for two static cultures for each strain are presented. Measurements were made at the Marine Biological Laboratory (Woods Hole, MA) with equipment loaned to the Microbial Diversity course.

SUPPLEMENTAL MATERIAL

Supplemental material for this article may be found at https://doi.org/10.1128/JB.00064-19.

SUPPLEMENTAL FILE 1, PDF file, 2.3 MB.
SUPPLEMENTAL FILE 2, MP4 file, 12.8 MB.
SUPPLEMENTAL FILE 3, MP4 file, 6.8 MB.
SUPPLEMENTAL FILE 4, MP4 file, 18.4 MB.

ACKNOWLEDGMENTS

I thank members of the Crosson lab for helpful discussions and feedback. Sean Crosson additionally provided valuable editorial feedback. The dissolved oxygen measurements were performed at the Marine Biological Laboratory (Woods Hole, MA) with equipment loaned to the Microbial Diversity course from Unisense. I thank Bingran Chen for her assistance in making these measurements.

This work was supported in part by a grant from the National Institutes of Health (R01GM087353).

REFERENCES

1. Davies JT, Rideal EK. 1963. Interfacial phenomena, 2nd ed. Academic Press, London, United Kingdom.
2. Van Oss CJ. 2006. Interfacial forces in aqueous media, 2nd ed, p 438. Taylor & Francis, Boca Raton, FL.
3. Marshall KC. 1996. Adhesion as a strategy for access to nutrients, p 59–87. *In* Fletcher M (ed), Bacterial adhesion: molecular and ecological diversity. Wiley-Liss, Inc., New York, NY.
4. Henrici AT. 1933. Studies of freshwater bacteria: I. A direct microscopic technique. J Bacteriol 25:277–287.
5. Zobell CE, Allen EC. 1935. The significance of marine bacteria in the fouling of submerged surfaces. J Bacteriol 29:239–251.
6. Naumann E. 1917. Beiträge zur kenntnis des teichnanoplanktons. II. Über das neuston des süßwasser. Biol Zentralbl 37:98–106.
7. Cunliffe M, Engel A, Frka S, Gasparovic B, Guitart C, Murrell JC, Salter M, Stolle C, Upstill-Goddard R, Wurl O. 2013. Sea surface microlayers: a unified physicochemical and biological perspective of the air-ocean interface. Prog Oceanogr 109:104–116. https://doi.org/10.1016/j.pocean.2012.08.004.
8. Cunliffe M, Upstill-Goddard RC, Murrell JC. 2011. Microbiology of aquatic surface microlayers. FEMS Microbiol Rev 35:233–246. https://doi.org/10.1111/j.1574-6976.2010.00246.x.
9. Wotton RS, Preston TM. 2005. Surface films: areas of water bodies that are often overlooked. Bioscience 55:137–145. https://doi.org/10.1641/0006-3568(2005)055[0137:SFAOWB]2.0.CO;2.
10. Kjelleberg S. 1985. Mechanisms of bacterial adhesion at gas-liquid interfaces, p 163–194. *In* Fletcher M, Savage DC (ed), Bacterial adhesion: mechanisms and physiological significance. Plenum Press, New York, NY.
11. Mills AL, Powelson DK. 1996. Bacterial interactions with surfaces in soils, p 25–57. *In* Fletcher M (ed), Bacterial adhesion: molecular and ecological diversity. Wiley-Liss, Inc, New York, NY.
12. Berne C, Ellison CK, Ducret A, Brun YV. 2018. Bacterial adhesion at the single-cell level. Nat Rev Microbiol 16:616–627. https://doi.org/10.1038/s41579-018-0057-5.
13. Davey ME, O'Toole GA. 2000. Microbial biofilms: from ecology to molecular genetics. Microbiol Mol Biol Rev 64:847–867. https://doi.org/10.1128/MMBR.64.4.847-867.2000.
14. Flemming HC, Wingender J, Szewzyk U, Steinberg P, Rice SA, Kjelleberg S. 2016. Biofilms: an emergent form of bacterial life. Nat Rev Microbiol 14:563–575. https://doi.org/10.1038/nrmicro.2016.94.
15. Vaccari L, Molaei M, Niepa THR, Lee D, Leheny RL, Stebe KJ. 2017. Films of bacteria at interfaces. Adv Colloid Interface Sci 247:561–572. https://doi.org/10.1016/j.cis.2017.07.016.
16. Armitano J, Mejean V, Jourlin-Castelli C. 2014. Gram-negative bacteria can also form pellicles. Environ Microbiol Rep 6:534–544. https://doi.org/10.1111/1758-2229.12171.
17. Okshevsky M, Meyer RL. 2015. The role of extracellular DNA in the establishment, maintenance and perpetuation of bacterial biofilms. Crit Rev Microbiol 41:341–352. https://doi.org/10.3109/1040841X.2013.841639.
18. Wilhelm RC. 2018. Following the terrestrial tracks of Caulobacter—redefining the ecology of a reputed aquatic oligotroph. ISME J 12:3025–3037. https://doi.org/10.1038/s41396-018-0257-z.
19. Poindexter JS. 1981. The caulobacters: ubiquitous unusual bacteria. Microbiol Rev 45:123–179.

20. Poindexter JS. 1964. Biological properties and classification of the Caulobacter group. Bacteriol Rev 28:231–295.
21. Stove JL, Stanier RY. 1962. Cellular differentiation in stalked bacteria. Nature 196:1189. https://doi.org/10.1038/1961189a0.
22. Poindexter JS. 2006. Dimorphic prosthecate bacteria: the genera Caulobacter, Asticcacaulis, Hyphomicrobium, Pedomicrobium, Hyphomonas and Thiodendron, p 72–90. *In* Dworkin M, Falkow S, Rosenberg E, Schleifer KH, Stackebrandt E (ed), The prokaryotes. Springer, New York, NY. https://doi.org/10.1007/0-387-30745-1_4.
23. Bodenmiller D, Toh E, Brun YV. 2004. Development of surface adhesion in Caulobacter crescentus. J Bacteriol 186:1438–1447. https://doi.org/10.1128/jb.186.5.1438-1447.2004.
24. Levi A, Jenal U. 2006. Holdfast formation in motile swarmer cells optimizes surface attachment during Caulobacter crescentus development. J Bacteriol 188:5315–5318. https://doi.org/10.1128/JB.01725-05.
25. Li G, Brown PJ, Tang JX, Xu J, Quardokus EM, Fuqua C, Brun YV. 2012. Surface contact stimulates the just-in-time deployment of bacterial adhesins. Mol Microbiol 83:41–51. https://doi.org/10.1111/j.1365-2958.2011.07909.x.
26. Entcheva-Dimitrov P, Spormann AM. 2004. Dynamics and control of biofilms of the oligotrophic bacterium Caulobacter crescentus. J Bacteriol 186:8254–8266. https://doi.org/10.1128/JB.186.24.8254-8266.2004.
27. Bowers LE, Weaver RH, Grula EA, Edwards OF. 1954. Studies on a strain of Caulobacter from water. I. Isolation and identification as Caulobacter vibrioides Henrici and Johnson with emended description. J Bacteriol 68:194–200.
28. Henrici AT, Johnson DE. 1935. Studies of freshwater bacteria: II. Stalked bacteria, a new order of Schizomycetes. J Bacteriol 30:61–93.
29. Smith CS, Hinz A, Bodenmiller D, Larson DE, Brun YV. 2003. Identification of genes required for synthesis of the adhesive holdfast in *Caulobacter crescentus*. J Bacteriol 185:1432–1442. https://doi.org/10.1128/jb.185.4.1432-1442.2003.
30. Toh E, Kurtz HD, Jr, Brun YV. 2008. Characterization of the Caulobacter crescentus holdfast polysaccharide biosynthesis pathway reveals significant redundancy in the initiating glycosyltransferase and polymerase steps. J Bacteriol 190:7219–7231. https://doi.org/10.1128/JB.01003-08.
31. Hershey DM, Fiebig A, Crosson S. 2019. A genome-wide analysis of adhesion in Caulobacter crescentus identifies new regulatory and biosynthetic components for holdfast assembly. mBio 10:e02273-18. https://doi.org/10.1128/mBio.02273-18.
32. Hershey DM, Porfírio S, Black I, Jaehrig B, Heiss C, Azadi P, Fiebig A, Crosson S. 2019. Composition of the holdfast polysaccharide from Caulobacter crescentus. J Bacteriol 201:e00276-19. https://doi.org/10.1128/JB.00276-19.
33. Hernando-Perez M, Setayeshgar S, Hou Y, Temam R, Brun YV, Dragnea B, Berne C. 2018. Layered structure and complex mechanochemistry underlie strength and versatility in a bacterial adhesive. mBio 9:e02359-17. https://doi.org/10.1128/mBio.02359-17.
34. Hentchel KL, Reyes Ruiz LM, Curtis PD, Fiebig A, Coleman ML, Crosson S. 2019. Genome-scale fitness profile of Caulobacter crescentus grown in natural freshwater. ISME J 13:523–536. https://doi.org/10.1038/s41396-018-0295-6.
35. Pamp SJ, Sternberg C, Tolker-Nielsen T. 2009. Insight into the microbial multicellular lifestyle via flow-cell technology and confocal microscopy. Cytometry A 75:90–103. https://doi.org/10.1002/cyto.a.20685.
36. O'Toole GA, Pratt LA, Watnick PI, Newman DK, Weaver VB, Kolter R. 1999. Genetic approaches to study of biofilms. Methods Enzymol 310:91–109. https://doi.org/10.1016/S0076-6879(99)10008-9.
37. Merker RI, Smit J. 1988. Characterization of the adhesive holdfast of marine and freshwater caulobacters. Appl Environ Microbiol 54:2078–2085.
38. Fiebig A, Herrou J, Fumeaux C, Radhakrishnan SK, Viollier PH, Crosson S. 2014. A cell cycle and nutritional checkpoint controlling bacterial surface adhesion. PLoS Genet 10:e1004101. https://doi.org/10.1371/journal.pgen.1004101.
39. Giltner CL, Nguyen Y, Burrows LL. 2012. Type IV pilin proteins: versatile molecular modules. Microbiol Mol Biol Rev 76:740–772. https://doi.org/10.1128/MMBR.00035-12.
40. Chaban B, Hughes HV, Beeby M. 2015. The flagellum in bacterial pathogens: for motility and a whole lot more. Semin Cell Dev Biol 46:91–103. https://doi.org/10.1016/j.semcdb.2015.10.032.
41. Yildiz FH, Visick KL. 2009. Vibrio biofilms: so much the same yet so different. Trends Microbiol 17:109–118. https://doi.org/10.1016/j.tim.2008.12.004.
42. Hug I, Deshpande S, Sprecher KS, Pfohl T, Jenal U. 2017. Second messenger-mediated tactile response by a bacterial rotary motor. Science 358:531–534. https://doi.org/10.1126/science.aan5353.
43. Ellison CK, Kan J, Dillard RS, Kysela DT, Ducret A, Berne C, Hampton CM, Ke Z, Wright ER, Biais N, Dalia AB, Brun YV. 2017. Obstruction of pilus retraction stimulates bacterial surface sensing. Science 358:535–538. https://doi.org/10.1126/science.aan5706.
44. Berne C, Ellison CK, Agarwal R, Severin GB, Fiebig A, Morton RI, III, Waters CM, Brun YV. 2018. Feedback regulation of Caulobacter crescentus holdfast synthesis by flagellum assembly via the holdfast inhibitor HfiA. Mol Microbiol 110:219–238. https://doi.org/10.1111/mmi.14099.
45. Ellison CK, Rusch DB, Brun YV. 4 March 2019. Flagellar mutants have reduced pilus synthesis in Caulobacter crescentus. J Bacteriol. https://doi.org/10.1128/JB.00031-19.
46. Marks ME, Castro-Rojas CM, Teiling C, Du L, Kapatral V, Walunas TL, Crosson S. 2010. The genetic basis of laboratory adaptation in Caulobacter crescentus. J Bacteriol 192:3678–3688. https://doi.org/10.1128/JB.00255-10.
47. Schrader JM, Shapiro L. 2015. Synchronization of Caulobacter crescentus for investigation of the bacterial cell cycle. J Vis Exp 98:52633. https://doi.org/10.3791/52633.
48. Ardissone S, Fumeaux C, Berge M, Beaussart A, Theraulaz L, Radhakrishnan SK, Dufrene YF, Viollier PH. 2014. Cell cycle constraints on capsulation and bacteriophage susceptibility. Elife 3:e03587. https://doi.org/10.7554/eLife.03587.
49. Fuerst JA, Mcgregor A, Dickson MR. 1987. Negative staining of freshwater bacterioneuston sampled directly with electron-microscope specimen support grids. Microb Ecol 13:219–228. https://doi.org/10.1007/BF02024999.
50. Tsang PH, Li G, Brun YV, Freund LB, Tang JX. 2006. Adhesion of single bacterial cells in the micronewton range. Proc Natl Acad Sci U S A 103:5764–5768. https://doi.org/10.1073/pnas.0601705103.
51. Hölscher T, Bartels B, Lin Y-C, Gallegos-Monterrosa R, Price-Whelan A, Kolter R, Dietrich LEP, Kovács ÁT. 2015. Motility, chemotaxis and aerotaxis contribute to competitiveness during bacterial pellicle biofilm development. J Mol Biol 427:3695–3708. https://doi.org/10.1016/j.jmb.2015.06.014.
52. Armitano J, Mejean V, Jourlin-Castelli C. 2013. Aerotaxis governs floating biofilm formation in Shewanella oneidensis. Environ Microbiol 15:3108–3118. https://doi.org/10.1111/1462-2920.12158.
53. Yamamoto K, Arai H, Ishii M, Igarashi Y. 2012. Involvement of flagella-driven motility and pili in Pseudomonas aeruginosa colonization at the air-liquid interface. Microbes Environ 27:320–323. https://doi.org/10.1264/jsme2.ME11322.
54. Giles SK, Stroeher UH, Eijkelkamp BA, Brown MH. 2015. Identification of genes essential for pellicle formation in Acinetobacter baumannii. BMC Microbiol 15:116. https://doi.org/10.1186/s12866-015-0440-6.
55. Morse M, Colin R, Wilson LG, Tang JX. 2016. The aerotactic response of Caulobacter crescentus. Biophys J 110:2076–2084. https://doi.org/10.1016/j.bpj.2016.03.028.
56. Crosson S, McGrath PT, Stephens C, McAdams HH, Shapiro L. 2005. Conserved modular design of an oxygen sensory/signaling network with species-specific output. Proc Natl Acad Sci U S A 102:8018–8023. https://doi.org/10.1073/pnas.0503022102.
57. Marshall KC, Cruickshank RH. 1973. Cell surface hydrophobicity and the orientation of certain bacteria at interfaces. Arch Mikrobiol 91:29–40. https://doi.org/10.1007/BF00409536.
58. Dahlback B, Hermansson M, Kjelleberg S, Norkrans B. 1981. The hydrophobicity of bacteria—an important factor in their initial adhesion at the air-water interface. Arch Microbiol 128:267–270. https://doi.org/10.1007/BF00422527.
59. Morse M, Huang A, Li G, Maxey MR, Tang JX. 2013. Molecular adsorption steers bacterial swimming at the air/water interface. Biophys J 105:21–28. https://doi.org/10.1016/j.bpj.2013.05.026.
60. Li G, Brun YV, Tang JX. 2013. Holdfast spreading and thickening during Caulobacter crescentus attachment to surfaces. BMC Microbiol 13:139. https://doi.org/10.1186/1471-2180-13-139.
61. Sommer JM, Newton A. 1988. Sequential regulation of developmental events during polar morphogenesis in Caulobacter crescentus: assembly of pili on swarmer cells requires cell separation. J Bacteriol 170:409–415. https://doi.org/10.1128/jb.170.1.409-415.1988.
62. Welker A, Cronenberg T, Zollner R, Meel C, Siewering K, Bender N, Hennes M, Oldewurtel ER, Maier B. 2018. Molecular motors govern liquidlike ordering and fusion dynamics of bacterial colonies. Phys Rev Lett 121:118102. https://doi.org/10.1103/PhysRevLett.121.118102.

63. Taktikos J, Lin YT, Stark H, Biais N, Zaburdaev V. 2015. Pili-induced clustering of N. gonorrhoeae bacteria. PLoS One 10:e0137661. https://doi.org/10.1371/journal.pone.0137661.
64. Higashi DL, Lee SW, Snyder A, Weyand NJ, Bakke A, So M. 2007. Dynamics of Neisseria gonorrhoeae attachment: microcolony development, cortical plaque formation, and cytoprotection. Infect Immun 75:4743–4753. https://doi.org/10.1128/IAI.00687-07.
65. Umbreit TH, Pate JL. 1978. Characterization of holdfast region of wild-type cells and holdfast mutants of Asticcacaulis-Biprosthecum. Arch Microbiol 118:157–168. https://doi.org/10.1007/BF00415724.
66. Maier B, Wong G. 2015. How bacteria use type IV pili machinery on surfaces. Trends Microbiol 23:775–788. https://doi.org/10.1016/j.tim.2015.09.002.
67. Persat A, Stone HA, Gitai Z. 2014. The curved shape of Caulobacter crescentus enhances surface colonization in flow. Nat Commun 5:3824. https://doi.org/10.1038/ncomms4824.
68. Matthysse AG. 1983. Role of bacterial cellulose fibrils in Agrobacterium tumefaciens infection. J Bacteriol 154:906–915.
69. Thompson MA, Onyeziri MC, Fuqua C. 2018. Function and regulation of Agrobacterium tumefaciens cell surface structures that promote attachment. Curr Top Microbiol Immunol 418:143–184. https://doi.org/10.1007/82_2018_96.
70. Berne C, Kysela DT, Brun YV. 2010. A bacterial extracellular DNA inhibits settling of motile progeny cells within a biofilm. Mol Microbiol 77:815–829. https://doi.org/10.1111/j.1365-2958.2010.07267.x.
71. Lagenaur C, Agabian N. 1978. Caulobacter flagellar organelle: synthesis, compartmentation, and assembly. J Bacteriol 135:1062–1069.
72. Fritts RK, LaSarre B, Stoner AM, Posto AL, McKinlay JB. 2017. A Rhizobiales-specific unipolar polysaccharide adhesin contributes to Rhodopseudomonas palustris biofilm formation across diverse photoheterotrophic conditions. Appl Environ Microbiol 83:e03035-16. https://doi.org/10.1128/AEM.03035-16.
73. Williams M, Hoffman MD, Daniel JJ, Madren SM, Dhroso A, Korkin D, Givan SA, Jacobson SC, Brown PJ. 2016. Short-stalked Prosthecomicrobium hirschii cells have a Caulobacter-like cell cycle. J Bacteriol 198:1149–1159. https://doi.org/10.1128/JB.00896-15.
74. Moore RL, Marshall KC. 1981. Attachment and rosette formation by hyphomicrobia. Appl Environ Microbiol 42:751–757.
75. Laus MC, Logman TJ, Lamers GE, Van Brussel AA, Carlson RW, Kijne JW. 2006. A novel polar surface polysaccharide from Rhizobium leguminosarum binds host plant lectin. Mol Microbiol 59:1704–1713. https://doi.org/10.1111/j.1365-2958.2006.05057.x.
76. Williams A, Wilkinson A, Krehenbrink M, Russo DM, Zorreguieta A, Downie JA. 2008. Glucomannan-mediated attachment of Rhizobium leguminosarum to pea root hairs is required for competitive nodule infection. J Bacteriol 190:4706–4715. https://doi.org/10.1128/JB.01694-07.
77. Xie F, Williams A, Edwards A, Downie JA. 2012. A plant arabinogalactan-like glycoprotein promotes a novel type of polar surface attachment by Rhizobium leguminosarum. Mol Plant Microbe Interact 25:250–258. https://doi.org/10.1094/MPMI-08-11-0211.
78. Tomlinson AD, Fuqua C. 2009. Mechanisms and regulation of polar surface attachment in Agrobacterium tumefaciens. Curr Opin Microbiol 12:708–714. https://doi.org/10.1016/j.mib.2009.09.014.
79. Xu J, Kim J, Koestler BJ, Choi JH, Waters CM, Fuqua C. 2013. Genetic analysis of Agrobacterium tumefaciens unipolar polysaccharide production reveals complex integrated control of the motile-to-sessile switch. Mol Microbiol 89:929–948. https://doi.org/10.1111/mmi.12321.
80. Loh JT, Ho SC, de Feijter AW, Wang JL, Schindler M. 1993. Carbohydrate binding activities of Bradyrhizobium japonicum: unipolar localization of the lectin BJ38 on the bacterial cell surface. Proc Natl Acad Sci U S A 90:3033–3037. https://doi.org/10.1073/pnas.90.7.3033.
81. Schaper S, Krol E, Skotnicka D, Kaever V, Hilker R, Sogaard-Andersen L, Becker A. 2016. Cyclic di-GMP regulates multiple cellular functions in the symbiotic alphaproteobacterium Sinorhizobium meliloti. J Bacteriol 198:521–535. https://doi.org/10.1128/JB.00795-15.
82. Chertkov O, Brown PJ, Kysela DT, de Pedro MA, Lucas S, Copeland A, Lapidus A, Del Rio TG, Tice H, Bruce D, Goodwin L, Pitluck S, Detter JC, Han C, Larimer F, Chang YJ, Jeffries CD, Land M, Hauser L, Kyrpides NC, Ivanova N, Ovchinnikova G, Tindall BJ, Goker M, Klenk HP, Brun YV. 2011. Complete genome sequence of Hirschia baltica type strain (IFAM 1418(T)). Stand Genomic Sci 5:287–297. https://doi.org/10.4056/sigs.2205004.
83. MacRae JD, Smit J. 1991. Characterization of caulobacters isolated from wastewater treatment systems. Appl Environ Microbiol 57:751–758.
84. Curtis PD. 2017. Stalk formation of Brevundimonas and how it compares to Caulobacter crescentus. PLoS One 12:e0184063. https://doi.org/10.1371/journal.pone.0184063.
85. Langille SE, Weiner RM. 1998. Spatial and temporal deposition of hyphomonas strain VP-6 capsules involved in biofilm formation. Appl Environ Microbiol 64:2906–2913.
86. Bruhn JB, Gram L, Belas R. 2007. Production of antibacterial compounds and biofilm formation by Roseobacter species are influenced by culture conditions. Appl Environ Microbiol 73:442–450. https://doi.org/10.1128/AEM.02238-06.
87. Bruhn JB, Nielsen KF, Hjelm M, Hansen M, Bresciani J, Schulz S, Gram L. 2005. Ecology, inhibitory activity, and morphogenesis of a marine antagonistic bacterium belonging to the Roseobacter clade. Appl Environ Microbiol 71:7263–7270. https://doi.org/10.1128/AEM.71.11.7263-7270.2005.
88. Slightom RN, Buchan A. 2009. Surface colonization by marine roseobacters: integrating genotype and phenotype. Appl Environ Microbiol 75:6027–6037. https://doi.org/10.1128/AEM.01508-09.
89. Frank O, Michael V, Pauker O, Boedeker C, Jogler C, Rohde M, Petersen J. 2015. Plasmid curing and the loss of grip—the 65-kb replicon of Phaeobacter inhibens DSM 17395 is required for biofilm formation, motility and the colonization of marine algae. Syst Appl Microbiol 38:120–127. https://doi.org/10.1016/j.syapm.2014.12.001.
90. Segev E, Tellez A, Vlamakis H, Kolter R. 2015. Morphological heterogeneity and attachment of Phaeobacter inhibens. PLoS One 10:e0141300. https://doi.org/10.1371/journal.pone.0141300.
91. Abraham WR, Estrela AB, Rohde M, Smit J, Vancanneyt M. 2013. Prosthecate sphingomonads: proposal of Sphingomonas canadensis sp. nov. Int J Syst Evol Microbiol 63:3214–3219. https://doi.org/10.1099/ijs.0.048678-0.
92. Min KR, Rickard AH. 2009. Coaggregation by the freshwater bacterium Sphingomonas natatoria alters dual-species biofilm formation. Appl Environ Microbiol 75:3987–3997. https://doi.org/10.1128/AEM.02843-08.
93. Yurkov V, Csotonyi JT. 2009. New light on aerobic anoxygenic phototrophs, p 31–55. *In* Hunter CN, Daldal F, Thurnauer MC, Beatty JT (ed), The purple phototrophic bacteria. Springer Netherlands, Dordrecht, Netherlands.
94. Gupta RS, Mok A. 2007. Phylogenomics and signature proteins for the alpha proteobacteria and its main groups. BMC Microbiol 7:106. https://doi.org/10.1186/1471-2180-7-106.
95. Xu J, Kim J, Danhorn T, Merritt PM, Fuqua C. 2012. Phosphorus limitation increases attachment in Agrobacterium tumefaciens and reveals a conditional functional redundancy in adhesin biosynthesis. Res Microbiol 163:674–684. https://doi.org/10.1016/j.resmic.2012.10.013.
96. Nierman WC, Feldblyum TV, Laub MT, Paulsen IT, Nelson KE, Eisen JA, Heidelberg JF, Alley MR, Ohta N, Maddock JR, Potocka I, Nelson WC, Newton A, Stephens C, Phadke ND, Ely B, DeBoy RT, Dodson RJ, Durkin AS, Gwinn ML, Haft DH, Kolonay JF, Smit J, Craven MB, Khouri H, Shetty J, Berry K, Utterback T, Tran K, Wolf A, Vamathevan J, Ermolaeva M, White O, Salzberg SL, Venter JC, Shapiro L, Fraser CM, Eisen J. 2001. Complete genome sequence of Caulobacter crescentus. Proc Natl Acad Sci U S A 98:4136–4141. https://doi.org/10.1073/pnas.061029298.